Chapter 6

Effective Performance Parameters of Piezoelectric Composites

6.1 Introduction

Advances in the sensors and actuator technology has been phenomenal in the last decade due to the development of new smart materials such as piezocomposites. These materials have an excellent property of converting energy from a mechanical domain to an electrical domain and vice-versa. This property of reciprocity in the energy conversion makes them a wonderful class of materials which have numerous applications in structural health monitoring, vibration, noise control, ultrasonic imaging, aerospace and avionics applications, aeroelastic control and underwater applications. These materials could be used to build many advanced structured systems incorporating their sensing and actuating capabilities which harness the coupled mechanical and electrical properties of piezocomposites demonstrating enhanced self-controlling and self-monitoring features. Since most often, these structures also sustain harsh conditions of thermoelastic fluctuations, their endurance to thermos-electro-elastic environment has been of concern and critical to the reliability of the smart piezoelectric structures.

In recent years, numerous analytical and numerical models have been developed for understanding the electromechanical properties of piezoelectric composites under different fiber volume fractions. Smith et. al., Chan *et. al.* and Crawley *et. al.* [16,101,143] have attempted to study the effective properties of piezoelectric composites using analytical models. Haun *et. al.* [13] developed an analytical model based on series and parallel connectivity for determining the piezoelectric and pyroelectric structure-property relations. Effective coefficients of piezoelectric ceramics with closed (0-3) and open (1-

3) pores has been evaluated analytically using a modified cubes model [19]. Adopting Eshelby's inclusion method, Dunn *et. al.* [26,32] proposed an analytical model to evaluate the effective electromechanical properties of piezoelectric composites using self-consistent scheme, differential scheme and Mori-Tanaka approximation. Based on the Mori-Tanaka theory and equivalent inclusion method, the author [91] presented analytical expressions to determine effective thermo-electro-elastic properties of the piezoelectric composites.

The effective properties of piezoelectric composites containing spatially oriented short fibers has also been studied by Huang *et. al.* [144] using an analytical unified method with three-dimensional coordinate transformation. Green's function technique has been extended by Nan *et. al.* [145] to study the effects of fiber volume fractions and ceramic rods/fibers orientation on the effective electro-elastic properties of 1-3 piezoelectric composites. Della *et. al.* [48] presented a micromechanics model based on the Mori-Tanaka method to study the performance of 1-3 piezoelectric composites with an active and passive matrix. It has been shown that the use of an active polymer matrix enhances the performance of such composites significantly, when compared with the use of a passive polymer matrix. The analysis of piezoelectric properties has also been carried out to determine the effective electro-elastic properties with strength of materials and method of cell approach. Shaktivel *et. al.* [130] adopted a micromechanics model based on classical mechanics theory to evaluate effective thermo-electro-elastic properties of 1-3 piezoelectric composites.

Analytical models discussed so far to evaluate the performance parameters of piezocomposites assume simplified parallel and transverse slab models ignoring the influence of fiber-packing geometry. However, in real composite structures not only fiber packings are random, but also loadings are multiaxial. Consequently, the simplified

mechanics of materials approach lead to susceptible smart structures. It can be concluded that analytical agreement with experimental results in the other transverse direction will be poor. Therefore, in the present work, analytical formulations in the light of a modified strength of materials (MSM) approach have been derived taking into account the effects of fiber packing arrangements for evaluating the effective piezo properties.

Apart from analytical models, in literature, numerical models have also been developed employing the unit-cell or representative volume element (RVE) to describe the constitutive behaviour of 1-3 piezoelectric composites. Numerical analyses based on finite element procedure using unit-cell and RVE model have been conducted to investigate the electro-elastic behaviour of piezoelectric composites with continuous and periodic alignment of fibers [65,121,122,135,146]. The overall effective electro-elastic coefficients for 0-3 and 1-3 piezoelectric composites are determined as a function of fiber volume fraction and fiber's aspect ratio. Bennett *et. al.* [136] developed a finite element model for thickness mode operations of 1-3 piezocomposite used commonly in hydrophone operations and studied the effects of the lateral pressures on such composites that typically occurs in a hydrostatic environment.

Effectively, both numerical and analytical techniques described do not address the coupled thermo-electro-elastic behaviour of 1-3 piezocomposites, where experimental data are also very limited and available for example problems only. Essentially, advancement of smart structure technology needs performance parameters to be more realistically simulated or derived. Necessitating from this research gap, hence the aim of the present investigations is stated as follows:

1. To develop an analytical model based on modified strength of materials approach to study the effective thermo-electro-elastic behavior of 1-3 piezocomposites.

2. Evaluation of the effective properties of 1-3 piezocomposites made of circular fiber rods embedded in soft polymer matrix employing Eshelby method and Mori-Tanaka approximation procedure.

The response performance parameters in terms of electromechanical coupling constant, acoustic impedance, stiffened longitudinal velocity, effective elastic coefficient in third direction for open and short-circuit state, pyroelectric coefficient and thermal coefficient are determined for different fiber volume fraction. The results obtained from MSM approach and Mori-Tanaka approximation are qualitatively compared with results obtained from analytical models based on classical mechanics of materials approach and relevant experimental results.

The work carried out in this chapter is organized as follows: the mathematical relations to describe coupled thermo-electro-elastic behaviour of a piezoelectric material is described in section 6.2. Based on modified strength of materials (MSM) approach, an analytical model is developed to evaluate effective thermo-electro-elastic coefficients of a 1-3 piezocomposite. An alternate analytical model based on Eshelby approach and Mori-Tanaka approximation is discussed in section 6.3. This model is adapted to evaluate effective thermo-electro-elastic coefficients of a 1-3 piezocomposite containing circular rods as fiber embedded in a soft polymer matrix. The parameters expressions on which performance of devices made up 1-3 piezocomposite depends, are discussed in section 6.4. The results obtained from the comparison of analytical models with measured experimental values [82] have been described in section 6.5 followed by conclusion in section 6.6.

6.2 Governing Equation of Piezoelectricity

The constitutive equations that govern the interaction of elastic, electric and the thermal fields in a thermo-electro-elastic medium is formulated as

$$\sigma_{ij} = C^{E}_{ijkl}\epsilon_{kl} - e_{ijk}E_k - \beta_{ij}\theta \tag{6.1a}$$

$$D_i = e_{ikl}\epsilon_{kl} + \kappa^{\varepsilon}_{ij}E_j + P_i\theta \tag{6.1b}$$

where σ_{ij} and ϵ_{kl} are the second rank stress and strain tensor, E_k, D_i and P_i are electric field vector, electric displacement vector and pyroelectric vector, respectively. C^{E}_{ijkl}, e_{ijk}, β_{ij} and κ^{ϵ}_{ij} denotes the fourth rank elastic stiffness tensor, the third rank piezoelectric tensor, the second rank thermal stress tensor and the second rank dielectric tensor, respectively. θ denotes the change in temperature. The superscript E and ε stand for the properties that are evaluated at zero or constant electric field and strain, respectively.

Following two-index notations as stated in [5], Eqn. 6.1 (a)-(b) can be restated as

$$\sigma_a = C^{E}_{ab}\epsilon_b - e_{ab}E_b - \beta_a\theta \tag{6.2a}$$

$$D_a = e_{ab}\epsilon_b + \kappa^{\varepsilon}_{ab}E_b + P_a\theta \tag{6.2b}$$

where the subscript a and b are derived from ij and kl as follows: for ij or kl = 11, 22, 33, 23, 13, 12 (e.g., $C_{1133} = C_{13}$), a and b corresponds to 1, 2, 3, 4, 5, 6 respectively. In compact notation, the stress (a) and strain tensor (b) can be represented in terms of indices 1, 2, 3, 4, 5, 6 (e.g., ε_{11}=ε_1, $2\varepsilon_{12} = \varepsilon_6$). Eqns. 6.2 (a)-(b) produces 21 elasticity, 18 piezoelectric, 6 permittivity, 6 thermal stress and 3 pyroelectric constants, i.e., a total of 54 independent material properties for characterization of a monolithic or composite piezoelectric material in a linear elastic domain. But, for the transversely isotropic symmetry conditions the number of independent coefficients reduces further to 13.

The 1-3 piezocomposite considered in the current analysis is made up of cylindrical piezoelectric ceramic rods embedded into a piezopolymer matrix as shown in Figure 6.1. As the 1-3 piezocomposite would show same materials symmetries as that of monolithic piezoceramic fiber, i.e., transversely isotropic, the constitutive equations can also be written as

$$\begin{bmatrix}\sigma_1^x\\ \sigma_2^x\\ \sigma_3^x\\ \sigma_4^x\\ \sigma_5^x\\ \sigma_6^x\\ D_1^x\\ D_2^x\\ D_3^x\end{bmatrix}=\begin{bmatrix}C_{11}^x & C_{12}^x & C_{13}^x & 0 & 0 & 0 & 0 & 0 & -e_{31}^x & -\beta_1^x\\ C_{12}^x & C_{11}^x & C_{13}^x & 0 & 0 & 0 & 0 & 0 & -e_{31}^x & -\beta_2^x\\ C_{13}^x & C_{13}^x & C_{33}^x & 0 & 0 & 0 & 0 & 0 & -e_{33}^x & -\beta_3^x\\ 0 & 0 & 0 & C_{44}^x & 0 & 0 & 0 & -e_{15}^x & 0 & 0\\ 0 & 0 & 0 & 0 & C_{44}^x & 0 & -e_{15}^x & 0 & 0 & 0\\ 0 & 0 & 0 & 0 & 0 & C_{66}^x & 0 & 0 & 0 & 0\\ 0 & 0 & 0 & 0 & e_{15}^x & 0 & \kappa_{11}^x & 0 & 0 & P_1^x\\ 0 & 0 & 0 & e_{15}^x & 0 & 0 & 0 & \kappa_{11}^x & 0 & P_2^x\\ e_{31}^x & e_{31}^x & e_{33}^x & 0 & 0 & 0 & 0 & 0 & \kappa_{33}^x & P_3^x\end{bmatrix}\begin{bmatrix}\epsilon_1^x\\ \epsilon_2^x\\ \epsilon_3^x\\ \epsilon_4^x\\ \epsilon_5^x\\ \epsilon_6^x\\ E_1^x\\ E_2^x\\ E_3^x\\ \theta^x\end{bmatrix} \tag{6.3}$$

The superscript x denotes c, f and m for the composite, the fiber and the matrix respectively when expressed in equation form, e.g., the normal stress in the direction-1 of fiber, matrix and composite can be expressed as

$$\sigma_1^f = C_{11}^f\epsilon_1^f + C_{12}^f\epsilon_2^f + C_{13}^f\epsilon_3^f - e_{31}^f E_3^f - \beta_1^f\theta^f \tag{6.4}$$

$$\sigma_1^m = C_{11}^m\epsilon_1^m + C_{12}^m\epsilon_2^m + C_{13}^m\epsilon_3^m - e_{31}^m E_3^m - \beta_1^m\theta^m \tag{6.5}$$

$$\sigma_1^c = C_{11}^c\epsilon_1^c + C_{12}^c\epsilon_2^c + C_{13}^c\epsilon_3^c - e_{31}^c E_3^c - \beta_1^c\theta^c \tag{6.6}$$

6.3 Modified Strength of Materials (MSM) Model

Figure 6.1 shows a schematic representation of a 1-3 piezoelectric composite lamina that consists of an array of parallel piezoceramic fiber rods embedded in a polymer matrix. The assumptions for the theoretical study are stated as follows:

i. The fibers are continuous, parallel and aligned in the longitudinal direction- x_3.

ii. A constant electric field is applied in the direction transverse to that of fiber direction and this produces the same electric field in both the fiber as well as the matrix.

iii. Temperature change is identical for both the matrix and the fiber materials.

iv. Perfect bonding along the fiber-matrix interface throughout the domain.

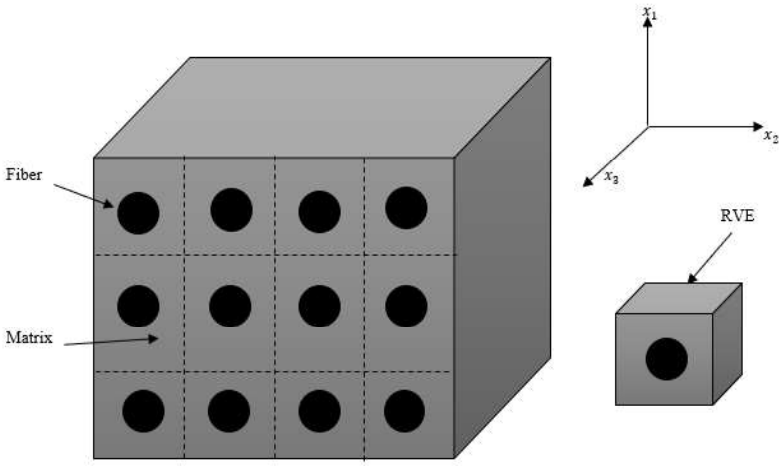

Figure 6.1 Schematic of a 1-3 piezoelectric composite.

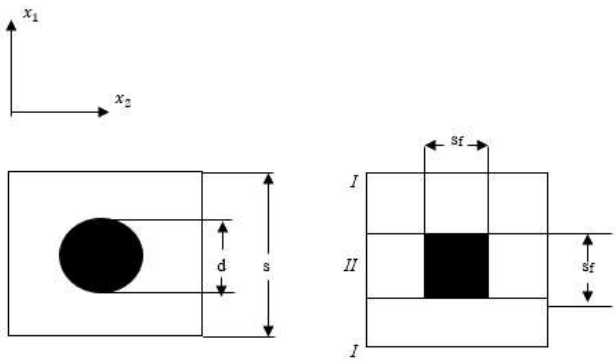

Figure 6.2 Transverse cross-section of a representative volume element (RVE) of 1-3 piezoelectric composite.

It is also worth noting that the elastic and piezoelectric coefficients of the constituent materials, i.e., of the fiber and the matrix are defined at the constant electric field. The bulk piezoelectric fiber reinforced composite can be visualized as an assembly of square representative volume elements (RVE) that contains both fiber and surrounding matrix materials. A repetitive arrangement of all RVEs shall constitute the whole piezoelectric material system. Figure 6.2 shows the transverse cross-section of such a representative volume element in a 1-3 piezocomposite. Taking the similar approach as discussed in section 5.3 of previous chapter and adding one more boundary condition related to change in temperature across the cross section of RVE; i.e., the change in temperature is also treated as same for the fiber, the matrix and the in direction-1, the thermal equilibrium is given as follows

$$\theta^c = \theta^f = \theta^m \tag{6.7}$$

The tedious manipulations and substitutions of coefficients similar to the approach adopted in deriving the analytical model discussed in Section 5.3 of previous chapter, the

effective thermo-electro-elastic coefficients of the piezoelectric composite can be expressed as follows:

$$C_{11}^c = \sqrt{v_f}\left(l_1 C_{12}^{fE} + m_1 C_{13}^{fE}\right) - \left(1-\sqrt{v_f}\right)\left(l_1' C_{12}^{mE} + m_1' C_{13}^{mE}\right) \tag{6.8}$$

$$C_{12}^c = \sqrt{v_f}\left(l_2 C_{12}^{fE} + m_2 C_{13}^{fE}\right) - \left(1-\sqrt{v_f}\right)\left(l_2' C_{12}^{mE} + m_2' C_{13}^{mE}\right) \tag{6.9}$$

$$C_{13}^c = \sqrt{v_f}\left(l_3 C_{12}^{fE} + m_3 C_{13}^{fE}\right) - \left(1-\sqrt{v_f}\right)\left(l_3' C_{12}^{mE} + m_3' C_{13}^{mE}\right) \tag{6.10}$$

$$\begin{aligned} C_{33}^c = {} & \sqrt{v_f} C_{33}^{fE} + \left(1-\sqrt{v_f}\right) C_{33}^{mE} + \sqrt{v_f}\left(l_3 C_{13}^{fE} + m_3 C_{33}^{fE}\right) \\ & - \left(1-\sqrt{v_f}\right)\left(l_3' C_{13}^{mE} + m_3' C_{33}^{mE}\right) \end{aligned} \tag{6.11}$$

$$e_{31}^c = \sqrt{v_f}\left(l_4 C_{12}^{fE} + m_4 C_{13}^{fE}\right) - \left(1-\sqrt{v_f}\right)\left(l_4' C_{12}^{mE} + m_4' C_{13}^{mE}\right) \tag{6.12}$$

$$\begin{aligned} e_{33}^c = {} & \sqrt{v_f} e_{31}^f + \left(1-\sqrt{v_f}\right) e_{31}^m + \sqrt{v_f}\left(l_4 C_{13}^{fE} + m_4 C_{33}^{fE}\right) \\ & - \left(1-\sqrt{v_f}\right)\left(l_4' C_{13}^{mE} + m_3' C_{33}^{mE}\right) \end{aligned} \tag{6.13}$$

$$\kappa_{11}^c = \sqrt{v_f}\left(l_4 e_{31}^f + m_4 e_{31}^f\right) + \left(1-\sqrt{v_f}\right)\left(l_4' e_{31}^m + m_4' e_{31}^m\right) \tag{6.14}$$

$$\begin{aligned} \kappa_{33}^c = {} & \sqrt{v_f}\kappa_{33}^{f\epsilon} + \left(1-\sqrt{v_f}\right)\kappa_{33}^{m\epsilon} - \sqrt{v_f}\left(l_4 e_{31}^f + m_4 e_{33}^f\right) \\ & + \left(1-\sqrt{v_f}\right)\left(l_4' e_{31}^m + m_4' e_{33}^m\right) \end{aligned} \tag{6.15}$$

$$\beta_1^c = \sqrt{v_f}\left(l_5 C_{13}^f + m_5 C_{33}^f\right) - \left(1-\sqrt{v_f}\right)\left(l_5' C_{13}^m + m_5' C_{33}^m\right) \tag{6.16}$$

$$\begin{aligned} \beta_3^c = {} & \sqrt{v_f}\beta_{33}^f + \left(1-\sqrt{v_f}\right)\beta_{33}^m + \sqrt{v_f}\left(l_5 C_{13}^f + m_5 C_{33}^f\right) \\ & - \left(1-\sqrt{v_f}\right)\left(l_5' C_{13}^m + m_5' C_{33}^m\right) \end{aligned} \tag{6.17}$$

$$P_1^c = \sqrt{v_f}\left(l_5 e_{131}^f + m_5 e_{33}^f\right) - \left(1-\sqrt{v_f}\right)\left(l_5' e_{31}^m + m_5' e_{33}^m\right) \tag{6.18}$$

$$\begin{aligned} P_3^c = {} & \sqrt{v_f} P_{33}^f + \left(1-\sqrt{v_f}\right) P_{33}^m - \sqrt{v_f}\left(l_5 e_{131}^f + m_5 e_{33}^f\right) \\ & + \left(1-\sqrt{v_f}\right)\left(l_5' e_{31}^m + m_5' e_{33}^m\right) \end{aligned} \tag{6.19}$$

The values of constants l_i, m_i, l_i' and m_i' (i ranges from 1 to 5) are described in terms of constituent material properties in the Appendix C.

6.4 Analytical Model based on Mori-Tanaka Approach

Dunn *et. al.* [26,32] proposed an analytical model to predict the effective coefficients of a piezoelectric composite by coupling the exact solution of an isolated ellipsoidal inclusion in a piezoelectric solid with a micromechanics approach i.e. effective medium approach. Based on Mori-Tanaka mean-field theory which accounts for the interaction between inclusions and the matrix, Huang [147] effectively applied these results to calculate effective thermo-electro-elastic coefficients of a piezoelectric composite as a function of fiber volume fraction, phase properties and inhomogeneity shape.

The constitutive relations shown in Eqns. 6.1 (a)-(b) may also be represented as

$$\Sigma_{iJ} = L_{iJMn} Z_{Mn} \tag{6.20}$$

where,

$$\Sigma_{iJ} = \begin{cases} \sigma_{ij} & J = 1,2,3 \\ D_i & J = 4 \end{cases} \tag{6.21}$$

$$Z_{Mn} = \begin{cases} \epsilon_{mn} & M = 1,2,3 \\ -E_n & M = 4 \end{cases} \tag{6.22}$$

$$L_{iJMn} = \begin{cases} C_{ijmn} & J, M = 1,2,3 \\ e_{nij} & J = 1,2,3; M = 4 \\ e_{imn} & J = 4; M = 1,2,3 \\ -\kappa_{in} & J, M = 4 \end{cases} \tag{6.23}$$

and,

$$\alpha_{Mn} = \begin{cases} \alpha_{mn} & M = 1,2,3 \\ P_n & M = 4 \end{cases} \tag{6.24}$$

In above equations, the uppercase subscript is summed over the range of 1-4 and the lower subscript is summed over the range of 1-3. Based on the equivalent inclusion method, the coupled electro-elastic fields in an inhomogeneity are expressed in terms of

four tensors. These tensors are piezoelectric analogue of Eshelby's tensor in elasticity [23] and are seen to be functions of the electro-elastic moduli of the matrix and the shape of the inclusion. The piezoelectric constraint tensors are represented as

$$S_{MnAb} = \begin{cases} \frac{a_1 a_2 a_3}{8\pi} L^m_{iJAb} \int_{|z|=1} \frac{1}{\zeta^3} \left[G_{MJin}(z) + G_{nJiM}(z)\right] ds(z), & M = 1,2,3 \\ \frac{a_1 a_2 a_3}{4\pi} L^m_{iJAb} \int_{|z|=1} \frac{1}{\zeta^3} G_{4Jin}(z) ds(z), & M = 4 \end{cases} \tag{6.25}$$

where a_1, a_2, and a_3 are semi-major axes of ellipsoidal inclusion and G are Green's functions.

The closed form solution of the constraint tensors shown in Eqn. (6.25) doesn't exist for an anisotropic material. However, for certain materials symmetry the integrals shown in Eqn. (6.25) does have closed form solutions. Based on Mori-Tanaka mean field approach, the effective electro-elastic coefficients can be represented as [147]

$$\bar{L}_{bAMn} = L^m_{bAPq}[I_{PqMn} + v_f U^{-1}_{PqiJ}\left(L^f_{iJMn} - L^m_{iJMn}\right)] \tag{6.26}$$

and the effective thermal expansion and pyroelectric coefficients can be represented as

$$\bar{\alpha}_{Ab} = \alpha^m_{Ab} + v_f V^{-1}_{PqiJ} L^f_{iJMn}(\alpha^f_{Ab} - \alpha^m_{Ab}) \tag{6.27}$$

where v_f is the volume fraction of fiber and superscript f and m refers to fiber and matrix phase, respectively. The overbar denotes the overall effective properties of the composite. The other terms used in Eqn. (6.26) and (6.27) are defined as

$$U_{iJAb} = [\left(1 - v_f\right)\left(L^f_{iJMn} - L^m_{iJMn}\right)(S_{MnAb} - I_{MnAb}) + L^f_{iJAb}] \tag{6.28}$$

$$V_{iJAb} = \left(1 - v_f\right)[L^f_{iJMn} - L^m_{iJMn}]S_{MnAb} + L^m_{iJAb} \tag{6.29}$$

and,

$$I_{MnAb} = \begin{cases} \frac{1}{2}(\delta_{am}\delta_{bn} + \delta_{an}\delta_{bm}) & A, M = 1,2,3 \\ 0, & A = 1,2,3; M = 4 \\ 0, & A = 4; M = 1,2,3 \\ \delta_{bn} & A, M = 4, \end{cases} \quad (6.30)$$

For the completeness of the solution, the components of the Eshelby tensors used for modelling 1-3 piezoelectric composite are provided in Appendix C.

6.5 Performance Parameters of 1-3 Piezocomposite

Characterizing parameters to study the performance of 1-3 piezoelectric composites for respective smart applications has been evaluated as a function of fiber volume fraction. For using the piezocomposite as underwater acoustic transducer or hydrophone, these parameters, i.e., hydrostatic charge coefficient d_h, hydrostatic voltage coefficient g_h, the hydrophone figure of merit (FOM) $d_h g_h$ and hydrostatic electromechanical coupling factor k_h determine the performance of the composite [48]. Similarly, if the piezocomposite is being used as a transducer for biomedical imaging applications, the electromechanical coupling coefficient k_t, the acoustic impedance Z and the stiffened longitudinal velocity, V_{33}^D measures the performance of the composite.

6.5.1 Piezoelectric Charge Coefficient

The piezoelectric charge coefficient $(d_h = d_{31} + d_{32} + d_{33})$ is a measure of effective strength of electromechanical coupling in a piezoelectric material under hydrostatic loading conditions. To detect sound waves in the hydrophone applications, a large value of piezoelectric charge coefficient is required for the detection of waves of very small wavelengths. The charge coefficient, h, relates to piezoelectric constants as

$$e_{nij} = d_{nkl} C_{klij}^E \quad (6.31)$$

6.5.2 Hydrostatic Electromechanical Coupling Factor

The hydrostatic electromechanical coupling factor k_h which measures the efficiency of conversion of acoustic power to electrical power when the device is being operated in a hydrostatic environment, is defined as

$$k_h^2 = \frac{d_h^2}{\kappa_{33} S_h} \tag{6.32}$$

where,

$$S_h = 2S_{11} + 2S_{12} + 4S_{13} + S_{33} \tag{6.33}$$

where S_{11}, S_{12}, S_{13}, S_{33} are the effective composite compliance constants obtained by taking the inverse of an effective composite stiffness matrix.

6.5.3 Electromechanical Coupling Constant

The electromechanical coupling coefficient k_t is defined as the efficiency of energy conversion between the electrical and mechanical domains; a system exhibiting values closer to 1 being more desirable. It is represented as

$$k_t = \sqrt{1 - \frac{C_{33}^E}{C_{33}^D}} \tag{6.34}$$

where,

$$C_{33}^D = C_{33}^E + \frac{e_{33}^2}{\kappa_{33}} \tag{6.35}$$

The C_{33}^D and C_{33}^E are respectively the open-circuit stiffness and short-circuit stiffness constants.

6.5.4 The Acoustic Impedance

The acoustic impedance Z is a parameter to measure the amount of acoustic energy transfer between two materials. Though for piezoceramics this value lies between 20-30 MRayls, it can be significantly improved for such composite structures where some of the dense and stiff ceramic is replaced with a less dense and more compliant polymer. It is defined as

$$Z = (C_{33}^{D}\rho)^{1/2} \tag{6.36}$$

6.5.5 Stiffened Longitudinal Velocity

The stiffened longitudinal velocity V_{33}^{D} is defined as,

$$V_{33}^{D} = \sqrt{\frac{C_{33}^{D}}{\rho}} \tag{6.37}$$

In the above equations, ρ is composite density and is defined as

$$\rho = v_f\rho_f + v_m\rho_m \tag{6.38}$$

where ρ_f and ρ_m denote the density of the fiber and the matrix and the open-circuit stiffness constant C_{33}^{D} is given as

$$C_{33}^{D} = C_{33}^{E} + \frac{e_{33}^{2}}{\kappa_{33}} \tag{6.39}$$

6.6 Results and Discussion

This section presents the comparison of results obtained from the theoretical solutions described in section 6.3, i.e., modified strength of materials (MSM) approach and Mori-Tanaka approximation [147] with the micromechanics-based models [132,138] and experimental results in published literature [82] This exercise also gives an insight into the deviation between micromechanics model and experimentation values. In the current study, the 1-3 piezoelectric composite made of cylindrical fiber embedded in a soft polymer matrix has been considered. The piezoelectric fiber chosen are of TLZ-5 ceramic, and the matrix is VDF/TrFE (75/25 mol %) copolymer. This piezocomposite typically possesses significant value of piezoelectric and pyroelectric coefficients as compared with other such materials. For calculation of effective properties of 1-3 piezocomposite from analytical methods the material properties of the constituent, i.e., of fiber and matrix has been referred from Table 1.

The fiber and the matrix are poled in the same direction and the fiber is aligned in x_3-direction longitudinally while the matrix surrounds the fiber from all three dimensions. The present study focuses on studying the influence of fiber volume fraction and constituent material properties on various performance parameters of 1-3 piezoelectric composites. The performance parameters or figures of merit have been estimated with various analytical models to analyse the effectiveness of the current model while predicting the numerical values. The Mori-Tanaka approximation technique is based on Eshelby tensors, the special case of these tensors especially derived for long piezoelectric fiber embedded in a matrix medium is stated in Appendix C.

Table 6.1 Material properties of constituents (fiber and matrix phases)

Material Prop.	TLZ-5	VDF/TRFE Copolymer
C_{11}^E	126 GPa	8.5 GPa
C_{12}^E	79.5 GPa	3.6 GPa
C_{13}^E	84.1 GPa	3.6 GPa
C_{33}^E	109 GPa	9.9 GPa
C_{33}^D	147 GPa	10.7GPa
C_{44}^E	23 GPa	1.9 GPa
C_{66}^E	23.5 GPa	2.458 GPa
e_{31}	-6.5 (C/m^2)	0.008 (C/m^2)
e_{33}	24.8 (C/m^2)	-0.29 (C/m^2)
e_{15}	17 (C/m^2)	-0.002 (C/m^2)
κ_{11}^{ϵ} , κ_{22}^{ϵ}	1.505×10^{-8} (C/Vm)	6.641×10^{-11} (C/Vm)
κ_{33}^{ϵ}	1.605×10^{-8} (C/Vm)	7.960×10^{-11} (C/Vm)
$\alpha_{11}, \alpha_{22}, \alpha_{33}$	1.2×10^{-6} ($^0C^{-1}$)	0.18×10^{-6} ($^0C^{-1}$)
P_1, P_2, P_3	2.5×10^{-5} ($C/K/m^2$)	2.0×10^{-5} ($C/K/m^2$)
ρ	7898 (Kg/m^3)	1880 (Kg/m^3)

The performance of the devices which employ 1-3 piezoelectric composite materials are characterized using few parameters discussed in Section 6.5. Figures 6.3-6.5 illustrate the device parameters such as the electromechanical coupling constant K_t, the acoustic impedance Z, and the stiffened longitudinal velocity V_{33}^D. The electromechanical coupling constant K_t is a parameter which measures the conversion efficiency between acoustic and electrical energies in piezoelectric materials.

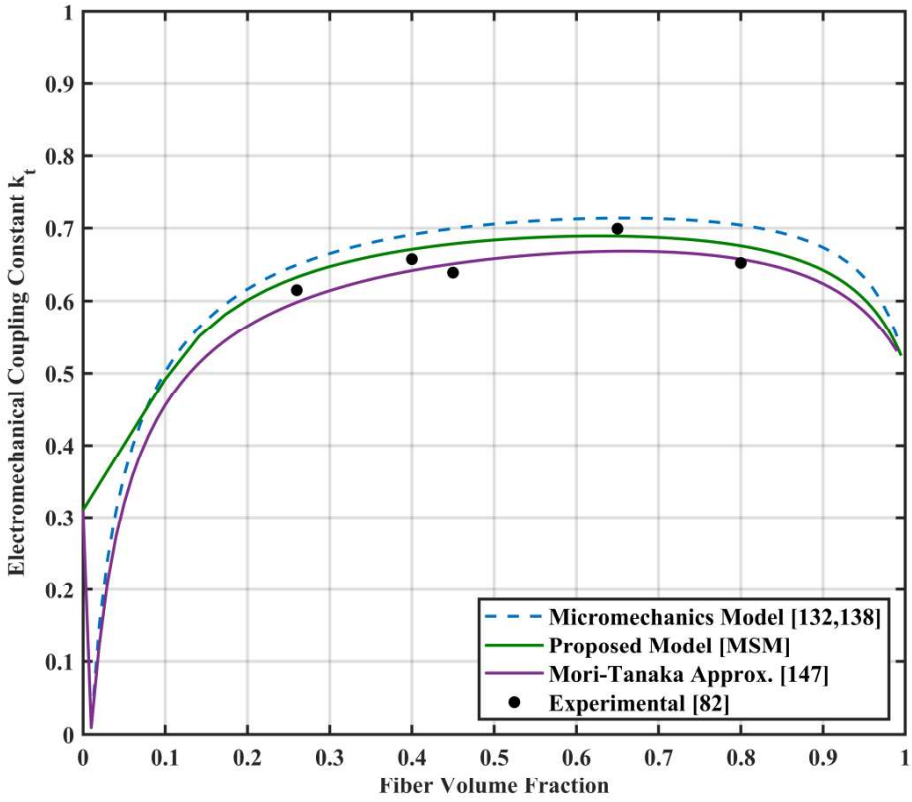

Figure 6.3 Comparison of effective electromechanical coupling constant K_t of 1-3 piezoelectric composite between experimental measurements and present analysis as a function of fiber volume fraction.

The value of K_t is found to increase rapidly and then attain almost 50% at about 0.1 volume fraction of the fiber as shown in Figure 6.3. Then it remains plateau at 70% along the mid-ranges of volume fraction and decreases towards the end of fiber volume fraction, i.e., 0.9-1.0. This can be reasoned that at low volume fractions, stiffening of the thin ceramic rods occurs due to the presence of large volume of surrounding polymer which increases K_t values and as the fiber volume fraction of the composite reaches nearer to pure ceramic state the lateral clamping of the ceramic fiber rods causes sharp decrease in

the value of K_t. Though the pattern of MSM model and Mori-Tanaka approximation exhibit a similar pattern to that of micromechanics model and experimental results, but individually they give an upper bound and lower bound of the distribution close to experimental data.

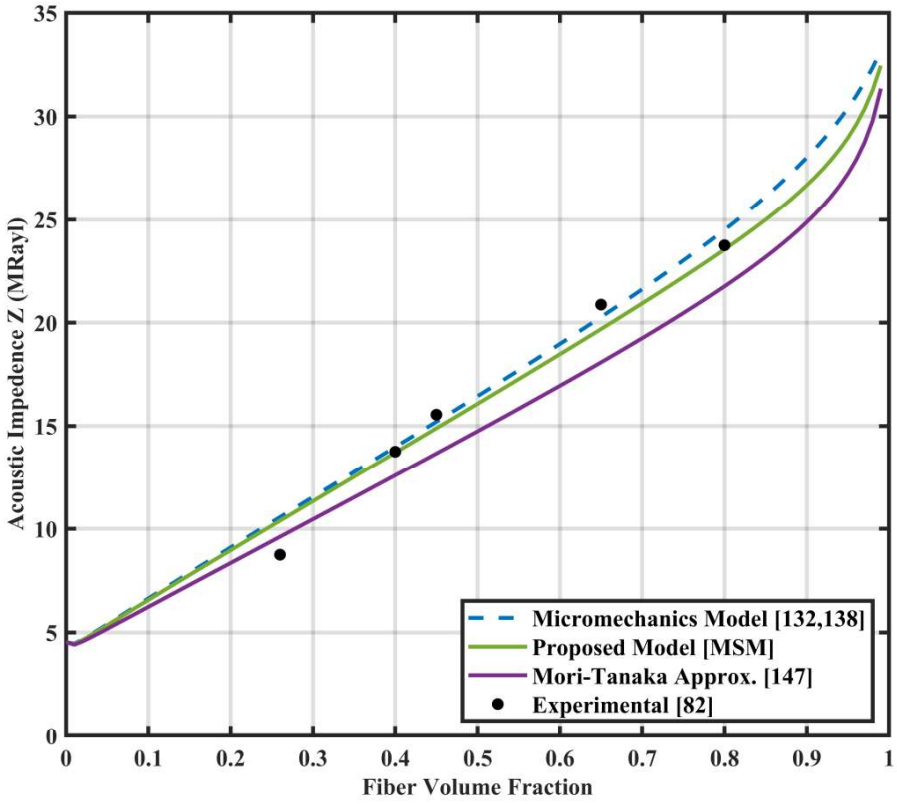

Figure 6.4 Comparison of effective acoustic impedance Z of 1-3 piezoelectric composite between experimental measurements and present analysis as a function of fiber volume fraction.

The acoustic impedance Z is a parameter which measures the transfer of acoustic energies between the two constituents, i.e., the fiber and the matrix of the composite. This is an essential design parameter for the development of devices meant for biomedical

applications where acoustic impedance of the structure needs to be matched with the human tissue. For the piezocomposites considered in the current study, this value is enhanced significantly as the less dense and more compliant polymer is replaced by some of the stiff and dense ceramic fiber materials. Figure 6.4 shows that the acoustic impedance increases linearly with increase in fiber volume fraction for almost the whole range of fiber volume fraction except there is some deviation reported at high end which may occur due to lateral clamping of the ceramic rods by the surrounding polymer. The MSM model is found to be in close agreement with the micromechanics and experimental models, whereas the Mori-Tanaka approximation deviates along the mid-range of volume fraction. This indicates that by proper tuning of the fiber volume fraction, appropriate design parameters can be achieved in practical applications.

Figure 6.5 shows an asymmetric variation of the parameter stiffened longitudinal velocity V_{33}^{D} for all the four models considered here, the variation being maximum for the experimental observations. The Mori-Tanaka approximation gives a lower bound, whereas the micromechanics model gives the upper bound with respect to fiber volume fraction. The predicted velocity parameter V_{33}^{D} increases with the fiber volume fraction and the gradients are stiff towards the high-end range of fiber volume fraction for all the theoretical models. This can be explained due to the stiffening of ceramic rods caused by the lateral forces imposed on them by the surrounding piezoelectric polymer at high fiber volume fraction.

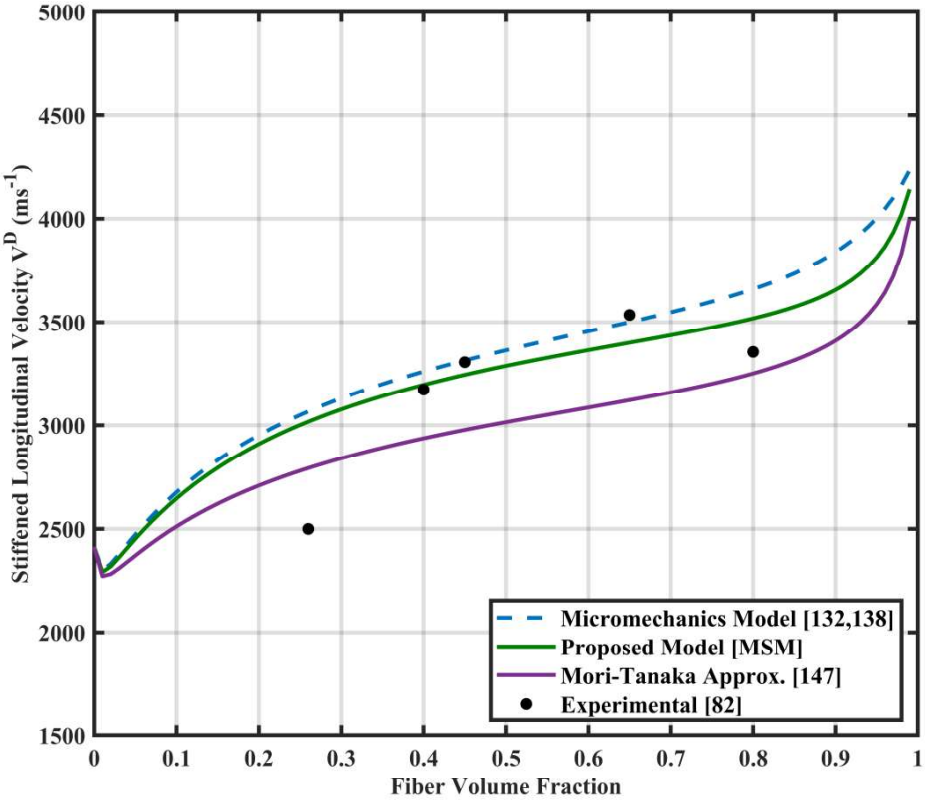

Figure 6.5 Comparison of effective stiffened longitudinal velocity V_{33}^{D} of 1-3 piezoelectric composite between experimental measurements and present analysis as a function of fiber volume fraction.

It can be observed from the curves shown in Figure 6.3-6.4 that predicted parameters of the 1-3 composite by analytical models discussed in section 6.3 agree quite well with the experimental results shown in the literature [82]. The stiffened longitudinal velocity V_{33}^{D} illustrated in Figure 6.5 suggests that experimental results are diverged at lower and higher ends of fiber volume fraction. Though curves show similar behaviour throughout the range of fiber volume fraction, it is worth noting that the values predicted with an analytical model given in the literature [132,138] and the value predicted with a model based on Mori-Tanaka approach forms upper and lower bounds respectively. The

model based on the modified strength of materials (MSM) approach discussed in section 6.4 predicts values within these bounds throughout the range of fiber volume fractions.

Depending upon a signal conditioning circuit between piezoelectric element and data acquisition system, the output of a piezoelectric sensor can be in open-circuit state and/or short-circuit state. If a charge amplifier is used for the excitation, the output obtained in data acquisition system will be termed as short-circuit state and if voltage amplifier is used for the excitation, then the output obtained will be termed as open-circuit state. When the electrodes of the composite are excited with these two distinct states, they give different stiffness values that render different sensor resonant frequencies.

Figures 6.6 and 6.7 show the variation in these two properties, i.e., C_{33}^{D} and C_{33}^{E} with respect to change in fiber volume fraction. All the theoretical models and experimental models are found to be in close agreement for a significant range of fiber volume fraction, though the Mori-Tanaka model gives a lower bound of the solution. Both the effective circuit parameters are found to vary almost linearly with fiber volume fraction initially with a sharp gradient and somewhat deviations from linearity towards the end for high volume fraction is observed. This may be attributed to the fact that at the high end of fiber volume fraction, lateral clamping of the ceramic rods occurs due to surrounding polymer which eventually alters the elastic behaviour of the composite. It is also observed from the simulation curves that the slope of short-circuit stiffness constant is more than open-circuit stiffness constant for the piezocomposites.

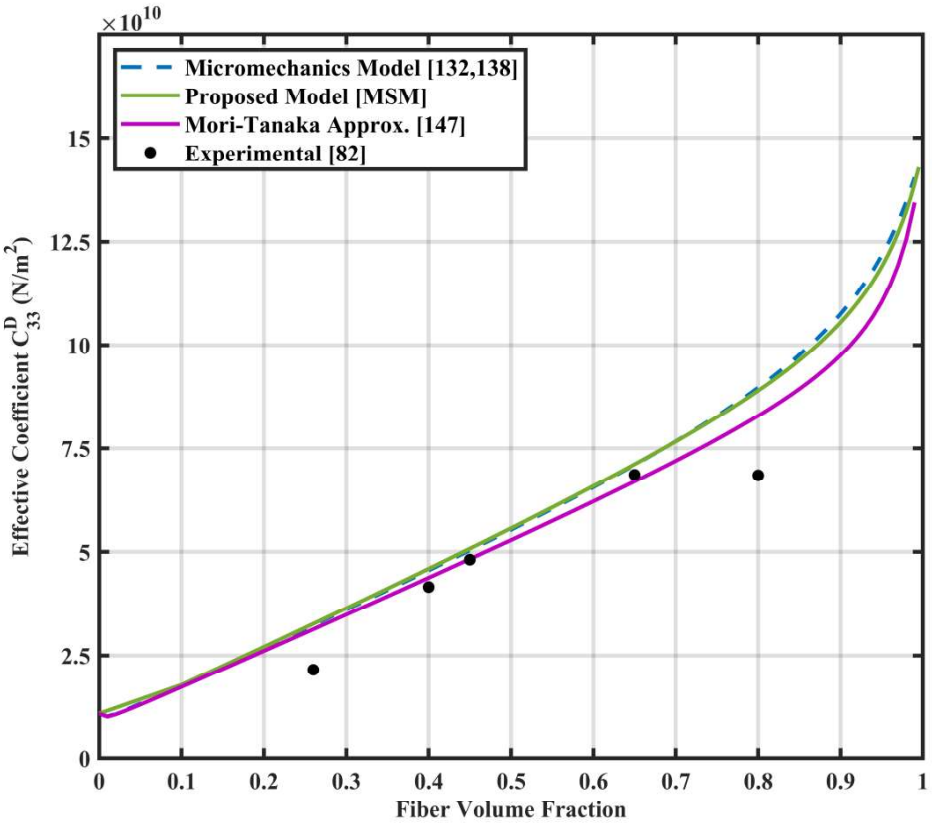

Figure 6.6 Comparison of effective short-circuit stiffness constant C_{33}^{D} of 1-3 piezoelectric composite between experimental measurements and present analysis as a function of fiber volume fraction.

It can be seen from Figures 6.6 and 6.7 that predicted parameters by model based on MSM approach shows quite resemblance with the analytical model of the literature [132,138] while model based on Mori- Tanaka approach [147] shows a huge underestimation of these two properties and forms the lower bound of the predicted values.

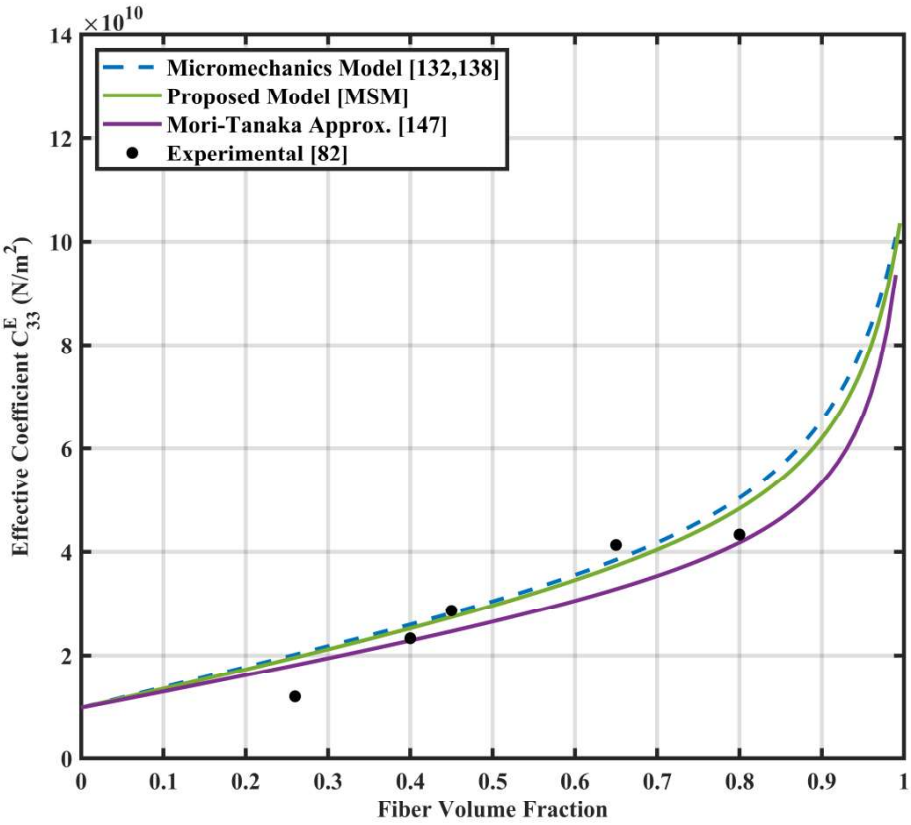

Figure 6.7 Comparison of effective short-circuit stiffness constant $C_{33}{}^{E}$ of 1-3 piezoelectric composite between experimental measurements and present analysis as a function of fiber volume fraction.

The effective hydrostatic charge coefficient d_h, is a very useful parameter to evaluate the performance of a device for underwater applications such as hydrophone. Figure 6.8 shows that the predicted value for the micromechanics model [132,138] gives highly overestimated results, whereas the experimental values [82] seems to be an underestimate of the variation. The values predicted by the model based on MSM approach and Mori-Tanaka approach [147] lie in between the two estimates. The maximum of charge coefficient $d_h$occurs between the 0.3 to 0.5 fiber volume fraction for all the models also the difference between the theoretical and experimental results are

significant for these regions. It is observed that the experimental values for the predicted charge coefficients are lower to the values predicted with all the analytical models for the entire range of fiber volume fraction.

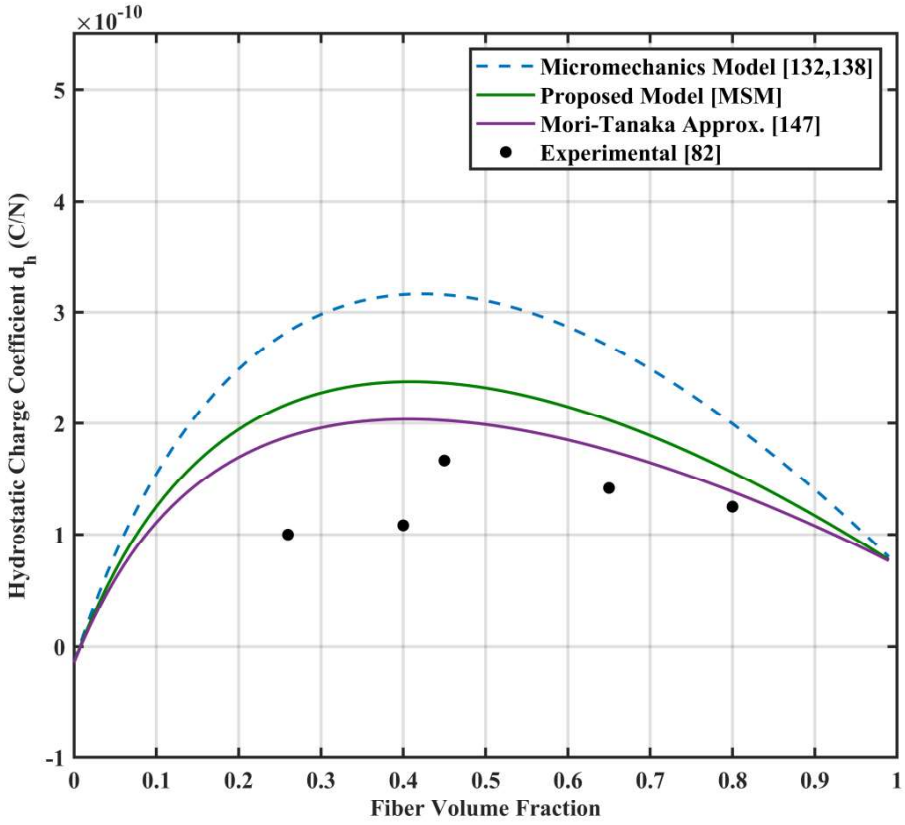

Figure 6.8 Comparison of effective hydrostatic charge coefficient d_h of 1-3 piezoelectric composite between experimental measurements and present analysis as a function of fiber volume fraction

The underestimation of the experimental estimation has already been partly explained in the literature [82] itself that the value of d_h depends strongly on the poling field. The huge underestimation of the measures value of d_h may be due to the fact that poling may have remained inadequate due to presence of the leakage resistance due to the

presence of pores that get developed during the synthetization of the piezocomposite. In addition to this, the frequency of the measurement also has significant effects on the measured value of d_h.

6.7 Summary

In this chapter, theoretical models in the light of a modified strength of materials (MSM) approach and Mori-Tanaka approximation scheme have been developed for predicting the performance characteristics of 1-3 piezoelectric composite subjected to a combined thermo-electro-mechanical loading. Mori-Tanaka approximation for evaluating the effective coefficients involves Eshelby's tensors solution for long fiber composites. Performance parameters for available experimental results have been compared with the three analytical models, i.e., micromechanics, modified strength of materials (MSM) and Mori-Tanaka models. The presented models are capable of predicting the effective coefficients with more precision than the existing models based on slab model or strength of materials model as the existing models neglect the randomness of fiber packing in real composite structures and coupled electro-elastic phenomena for piezocomposites in a uniaxial loading environment.

The comparison of results shows that the values predicted with micromechanics model forms the upper bound and the Mori-Tanaka estimation forms the lower bound for most of the performance parameters except for hydrostatic charge coefficient and pyroelectric coefficient. The theoretical calculations with modified strength of materials (MSM) model attains values within these bounds throughout the range of fiber volume fraction. The current study also leads to an important conclusion that the value of hydrostatic charge coefficient d_h is overpredicted by the analytical micromechanics model of the literature. It is evident from the comparison plots that the models based on

modified strength of materials (MSM) approach and Mori-Tanaka approach predict much closer values than the measured parameters employing experimental methods due to the presence of pores during preparation and curing of piezocomposite inducing leakage resistance. However, it is understood that some experimental fallacies are very difficult to avoid in development of piezo-systems leading to experimental errors as discussed in literature elsewhere. An inference can be drawn thus that the presence of active phase of both fiber and matrix in the composites provides better performance of the 1-3 piezocomposite than its monolithic counterpart, i.e., pure piezoelectric ceramic.

The predictions obtained from the derived models correlate well with the micromechanics model and existing experimental estimations. Though the upper and lower bound are different for some derived constants: electromechanical coupling constant, acoustic impedance, stiffened longitudinal velocity, effective elastic coefficient in third direction for open and short-circuit state, pyroelectric coefficient and thermal coefficient, but the asymptotic pattern remain similar for different fiber volume fraction. These parameters are important for the practical application of piezocomposite in smart structures either as sensors or actuators. From the ongoing analysis, it is believed that the theoretical models developed in this work can be extended for the design of large-scale integrated smart structures involving the thermo-electro-elastic behaviour of other composites subjected to more complex boundary conditions for critical high-risk applications.

Chapter 7

Conclusions and Suggestions for Future Work

7.1 General Conclusions

In the present thesis, the effective coefficients and performance parameters of both short and long fiber piezoelectric composite as a function of fiber shape and orientation were investigated. The study presents three micromechanics models, i.e., equivalent inclusion model, modified strength of materials (MSM) model and strain energy model. FEM based numerical analysis is also carried out to validate the proposed analytical models for both long and short-fiber piezocomposites. A more unified mathematical framework is developed to evaluate effective electromechanical coefficients across various length scales and geometries of the inclusion and/or inhomogeneity. To begin with, the exact solutions for the coupled electroelastic Green's functions are derived and the spatial distribution of electroelastic responses due to presence of an inclusion and/or inhomogeneity is studied. From the explicit expressions of Green's functions, it appears that they could be zero when the material is uncoupled. From the spatial distribution plots of Green's functions, it is clear that the distributions of different Green's functions are very similar while the magnitude varies significantly.

To study short fiber composites, by extending the results of classic Eshelby's solution of elasticity, a micromechanics model was derived for mapping electroelastic response of piezocomposites. The set of four constraint tensors, viz. Eshelby tensors that represented the stress and electric displacement of transformed inclusion from the surrounding matrix were derived for spheroid piezoelectric inclusion. The explicit expressions for the key component of these tensors, viz. electroelastic Green's functions

were derived and its spatial distribution as a function of fiber geometry was studied. Further, expressions to evaluate effective electroelastic coefficients (elastic, piezoelectric and dielectric) of piezocomposites were derived with two sets of boundary conditions: traction-electric displacement prescribed and elastic displacement-electric field prescribed. The effective electroelastic coefficients were estimated for various fiber shapes and geometries.

A finite element method (FEM) based analysis was carried out to study the effective properties of short fiber piezocomposites containing spheroid fiber inclusion. The problem was studied for two possible sets of fiber arrangements, i.e., SC and BCC. The effective elastic, piezoelectric and dielectric coefficients were calculated with finite element-based software ANSYS. The outcome of this analysis was later used to validate the results obtained through the proposed micromechanics model for short fiber composite developed earlier. An improved approach was developed to simulate the boundary conditions of the piezoelectric inclusion problem and special emphasis was given to capture the local field fluctuations of such problems.

To study the overall properties of long fiber composite, a micromechanics model was proposed to capture the effect of irregularity of fiber geometry and packing arrangement on transverse modulus of piezocomposites. Special consideration was made to capture the effects of transverse loading conditions on the overall properties of such piezocomposites. Exact solutions in the form of expressions were derived with a new approach developed with certain modifications in strength of materials (SM) approach (reported in the literature). Another analytical model is also developed based on the strain energy approach to check the validity of the modified model. The key parametric constants for strain energy methods remained the same specifically to validate the modified strength of materials (MSM) model. Later, a finite element method (FEM) based

approach was developed to study long fiber composites where special emphasis was given to the development of computer programmes to simulate periodic boundary conditions effectively. The effective electroelastic coefficients were calculated with FE software ANSYS for discrete fiber volume fractions. These FEM based calculated results were later used to validate the proposed micromechanics model, i.e., modified strength of materials (MSM) model.

In later parts, the performance parameters characterizing such piezocomposites were studied in the light of developed models. The figure of merits, e.g., hydrostatic charge coefficient d_h, the electromechanical coupling factor k_t, the acoustic impedance Z, stiffened longitudinal velocity V_{33}^D were calculated through modified strength of materials (MSM) model and Mori-Tanaka approximations using Eshelby model. Later, numerical results were validated with the experimental results to check the validity of the proposed models and also effectiveness and accuracy of the models to estimate performance parameters of such piezocomposites applications.

7.2 Suggestions for Future Work

1. Multiscale modeling of active composite allows integrating micromechanical models with several types of elements within finite element (FE) analysis, which will be useful for analyzing more complex structures made of active composites. The multiscale analysis is very useful for designing smart devices (structures) having active composites.

2. Constitutive modeling of multifunctional composite materials with coupled multiple physical responses, e.g., mechanical, electrical, thermal, magnetic, and optical, can be realized by integrating different constitutive models into the developed micromechanics model. This extension is very useful for studying different responses of numerous multifunctional composites.